Seismic Profiler and Sonobuoy Measurements in Ross Sea, Antarctica[1]

R. HOUTZ

Lamont-Doherty Geological Observatory of Columbia University
Palisades, New York 10964

F. J. DAVEY

Geophysics Division, Department of Scientific and Industrial Research
Wellington, New Zealand

Seismic profiler data from the continental shelf of the Ross Sea show numerous areas where gently dipping sediments with a total thickness of about 2 km are truncated at the sea floor or a few hundred meters below the sea floor. A series of basement (5.5 km/sec) 'highs,' which outcrop at the sea floor in the south and lie approximately along the 180th meridian, separates the shelf into two regions. Iselin bank lies on the northern extension of this line. The profiler and sonobuoy data show that the eastern shelf is formed by a sedimentary basin containing up to 4 km of sediments. The western shelf is more complex. Profiler data indicate gentle synclines and anticlines that plunge northward and overlie, in the south, older structures that trend ENE. Sonobuoy data from the shelf show a sharp increase in the sediment thickness in an elongate region parallel to 177°E. The increase in sediment thickness, caused possibly by the presence of N-S faulting, is not apparent in the profiler data. Over the whole shelf sonobuoy results show a linear increase in sediment velocity with depth. The geological trends seen on the shelf are not consistent with the northwesterly regional strikes mapped in Victoria Land or in western Marie Byrd Land. The continental rise in the east is marked by a sharp seaward increase in the basement depth, from about 4.5 to 6.5 km, at the base of the rise. In contrast, the western sector of the continental rise is more complex with basement ridges, whereas the depth to basement does not drop below about 4.5 km.

Geophysical data have been collected along 24,000 km of track in the Ross Sea during *Eltanin* cruises 27, 32, and 52. Profiler and magnetometer data were obtained on all the cruises, gravity data on cruises 32 and 52, and refraction and variable angle reflection data (using sonobuoys) only from cruise 52. PDR data are available from all cruises, including cruise 51, which otherwise undertook no geophysical observations. All these *Eltanin* cruises employed satellite navigation. The ship's tracks and location map appear in Figure 1*a*, and the bathymetry of the area is shown in Figure 1*b*. The bathymetry was taken from D. E. Hayes and F. J. Davey (in preparation, 1973) and is based almost exclusively on *Eltanin* data, which provided excellent coverage of the shelf and superior navigational control.

The sea floor of the Ross continental shelf is gently undulatory, consisting of a series of ridges trending NNE. It has a mean depth of approximately 500 meters. The seaward edge of the shelf, with the exception of the region of Iselin bank, follows almost a straight line connecting the northernmost parts of Victoria Land and Marie Byrd Land. The southern half of the Ross continental shelf is covered by the Ross ice shelf. Knowledge of the sea floor topography beneath this floating ice shelf is based on relatively few measurements, but near its edge the sea floor reflects a morphology similar to that of the sea floor in the uncovered parts of the continental shelf. The continental rise, especially in the western sector, is steep and irregular as a result of complicated faulting that occurs within the basement rocks of the rise. Note that 'continental rise,' as used in this paper,

[1] Lamont-Doherty Geological Observatory contribution 1963.

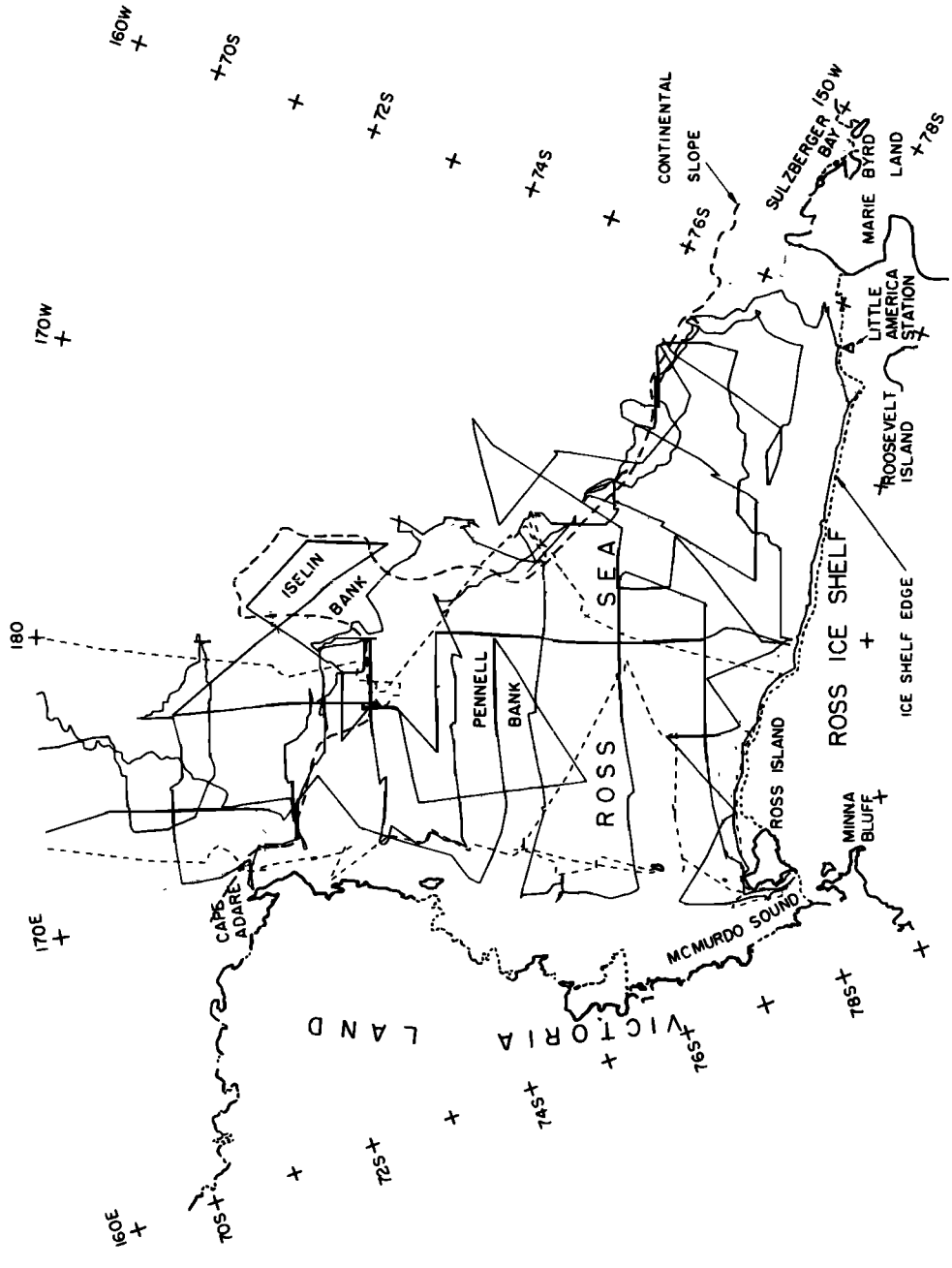

Fig. 1a. Location map. Tracks of *Eltanin* cruises 32 and 52 are shown by a solid line, cruise 27 by a dasned line, and cruise 51 by a dotted line.

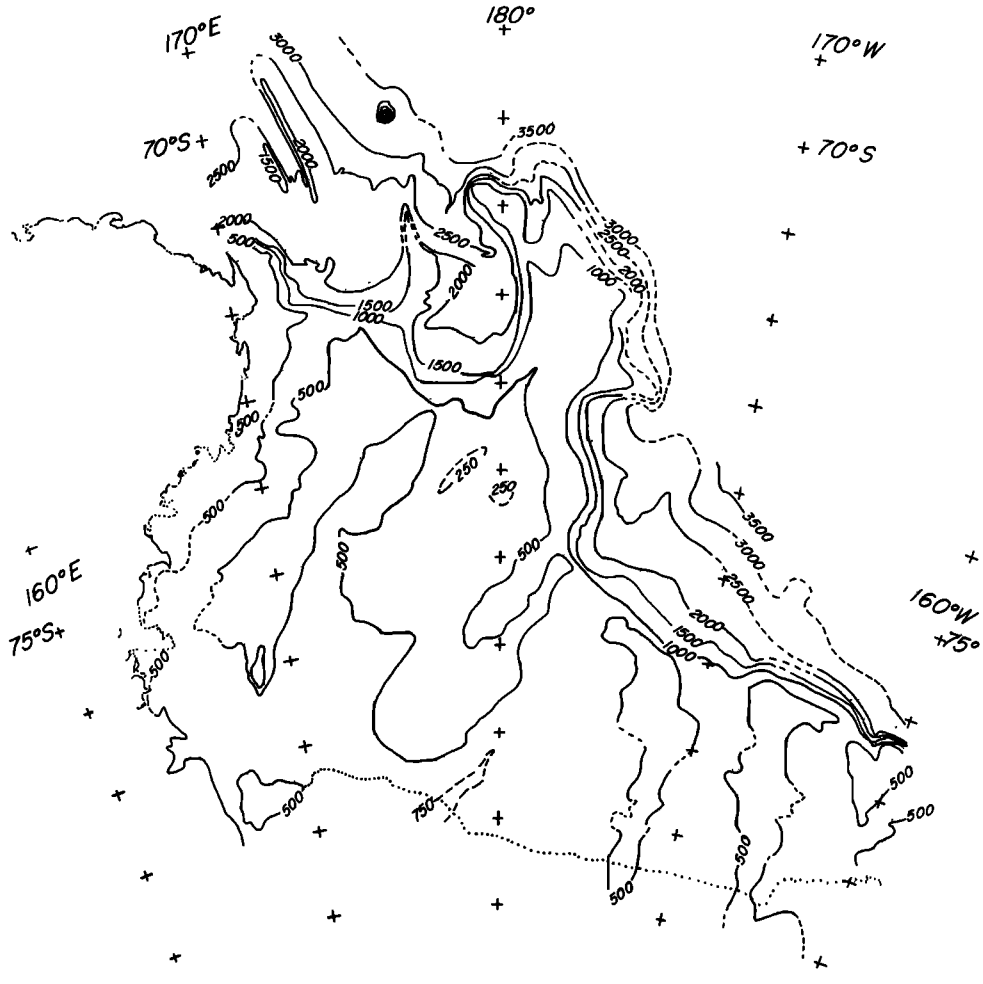

Fig. 1b. Generalized bathymetry of Ross Sea from D. E. Hayes and F. J. Davey (in preparation, 1973). Contours in meters corrected for variation of sound velocity in sea water after *Matthews* [1939].

refers to topography seaward of the shelf break that is too steep for a rise and too flat for a slope, according to the usual definitions (see Figures 11 and 14).

Earlier work by *Houtz and Meijer* [1970] revealed fold structures on the shelf radiating roughly outwards from the McMurdo Sound area. The present work modifies that structural picture somewhat and reveals important unconformities on the shelf. The application of the sonobuoy technique to the Ross shelf has greatly augmented our previous knowledge of the area by identifying basement rocks and by measuring the thickness of the sedimentary overburden on basement.

With one exception, other geophysical work in the area has been concentrated on the Ross ice shelf. *Crary* [1962] has presented some important seismic results for Little America station showing the existence of three layers with seismic velocities of 2.4, 4.24, and 6.4 km/sec, respectively. The low-velocity layer has a thickness of over 1300 meters, and the 4.24-km/sec layer, tentatively associated by Crary with the Beacon sandstone in southern Victoria Land, has a thickness of about 600 meters. Crary suggested that similar thick sedimentary rocks may be expected to underlie most of the Ross Sea and Ross ice shelf, a conclusion similar to that reached by *Adams and Christoffel* [1962]

who, from the lack of large-amplitude small-wavelength total force magnetic anomalies over the Ross Sea, postulated a considerable thickness of presumably sedimentary rocks. Gravity and magnetic observations carried out over the Ross ice shelf have been interpreted by *Bennett* [1964], the interpretation being based mainly on Crary's seismic results. Bennett concluded that the thick low-velocity sediments probably extend from Little America station at least halfway to the Transantarctic Mountains south of Victoria Land. It is apparent that, apart from the work of Houtz and Meijer, little is known about the detailed structure of the shelf.

EXTENT OF ICE SHELF DURING QUATERNARY TIMES

With some exceptions, early workers considered that the Ross shelf was covered with ice that was either grounded or floating at least during the last major glacial epoch. It was thought that Pennell bank (Figure 1*a*) is a terminal moraine, and hence much of the relatively rugged shelf topography was ascribed to morainal deposition. Terminal moraines are known in Sulzberger Bay [*Lepley*, 1966] and in the Ross Sea near McMurdo Sound [*Denton et al.*, 1970]. *Chriss and Frakes* [1973] have identified tillites on the continental rise. *Houtz and Meijer* [1970] showed from profiler records that Pennell bank was not morainal and found no evidence of morainal deposits or ice erosional forms at distances greater than about 80 km from the present edge of the ice shelf. They questioned whether the ice had ever covered the whole of the shelf.

The present work provides data that extend the observed northward limit of grounded ice to within 70 km of the shelf break, making it reasonably certain that the ice reached to the shelf edge at some earlier time, at least in the eastern Ross Sea. A photocopy of the reflection profile of a presumed morainal structure (section A-A′) appears in the upper part of Figure 2. In the section it appears as an isolated poorly layered mound resting on a flat sea floor. All sections are located in Figure 5. Well-identified zones of glacial erosion have modified the bathymetry parallel to and relatively near the ice shelf west of 180°, but the zones of erosion swing northward east of 180° as shown in Figure 6.

Poorly defined glacial(?) erosion from the western side of the shelf is illustrated in the lower part of Figure 2 (section B-B′). This section is across the channellike feature that passes to the west of Pennell bank and trends NNE. Elsewhere in the region west of 180° the supposed channels are less distinct. The apparent absence of morainal deposits west of the 180th meridian casts some doubt on these channellike features being glacial in origin. Alternatively, they could be the result of the scouring action of bottom currents, which are known to be strong on the Ross shelf [*Jacobs et al.*, 1970].

It is not possible from our data to confirm that the floating ice shelf formerly spread to the continental slope. The previous northward extent depends greatly on such unknown factors as former melt rates at the base of the ice shelf and ice flow onto the shelf from the Antarctic interior. If it did extend across the shelf, it would probably have grounded on the shoals underlying the western Ross Sea. *Hollin* [1962] has noted that existing Antarctic ice shelves are on the average at least 250 meters thick. It is therefore probable that, if an ice shelf existed across the Ross Sea during the Pleistocene, when the sea level was possibly 150 meters lower, it would have grounded in the western Ross Sea, where present water depths are less than 350 meters (assuming that rebound from the former load is now equilibrated). Pennell bank and two shoals nearby, one 200 km south

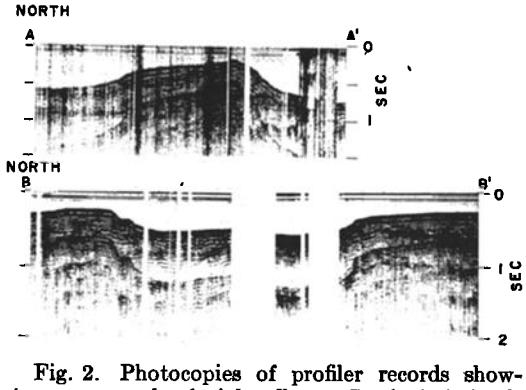

Fig. 2. Photocopies of profiler records showing presumed glacial effects. Section A-A′ is across a morainal feature, and section B-B′ illustrates possible glacial erosion or the effects of bottom current scour.

and one 200 km west of Pennell bank, are at shallower depths than this. The ice shelf over these banks could have been in a situation similar to that now over Roosevelt Island (that is, an isolated grounding) or it may have been part of a general grounding of the ice shelf arising from an increase in ice thickness due to the constriction in ice flow caused by the shelf grounding on the western banks. Supporting evidence for the latter case is suggested by the glacial history in the 'dry valleys' of southern Victoria Land. Ice advances from the east have been detected leaving glacial deposits at over 400 meters above sea level. These advances are suggested to have been associated with ice surface elevations in excess of 1000 meters in McMurdo Sound; hence a total ice thickness of about 2000 meters existed there, and these ice sheets were considered to extend at least 100 km to the north [*Calkin*, 1971]. The age of the maximum advance of the ice from the Ross Sea into the dry valleys, corresponding to the Pecten glaciation of *Calkin* [1971] and the Ross IV of *Denton et al.* [1970], occurred between 0.8 and 1.2 m.y. ago. This would correspond to the lowering of sea level in the Kansas, about 1–1.4 m.y. ago, of at least 150 meters [*Calkin*, 1971]. In Marie Byrd Land *Le Masurier* [1973] has suggested that the ice cover over the coastal regions could have been 1000 meters greater during the last glacial epoch than at present, thus tending to support the presence of an ice shelf over the entire Ross Sea. One possible effect of an increase in ice cover and grounding of the ice sheet in the western Ross Sea would be an increase in ice flow or subice water currents across the eastern Ross Sea resulting perhaps in the removal of up to 300 meters of sediments in this area, as will be discussed later. *Chriss and Frakes* [1973] have noted a bathymetric rise at the shelf edge. This corresponds to an increase in thickness of younger sediments (Figure 11, section L-L′) and may mark the edge of the former ice shelf.

ANALYSIS OF SONOBUOY DATA

Only three or four of the 23 sonobuoys deployed on the shelf recorded well-defined refraction lines composed of straight-line segments. All the remaining sonobuoys, except for a few from areas where the sediment cover is very thin, reveal pronounced curvature in the travel time data. Some examples of sonobuoys with nonlinear travel time curves appear in Figures 3*a* and 3*b*. Sonobuoy travel time data often show this kind of curvature as well as variations between straight-line segments and curves. The 'staircase' and continuous velocity models represent extremes, as discussed by *Bryan and Simpson* [1971], who observed both kinds as well as intermediate cases in their data from the coast of southwest Africa. *Eldholm and Ewing* [1971] established linear velocity functions in the Barents Sea by applying the Wiechert-Herglotz-Bateman integral to curved travel time data from individual sonobuoy records.

We wish to determine whether each sonobuoy record with curved travel time data represents a unique velocity function or if the entire shelf can be generalized by one function or regional functions. To find this out, we first obtained solutions by fitting artificial straight lines to the sonobuoy travel time curves. Solutions were then obtained in the usual way from the slopes and intercepts on the assumption of constant velocity layers. The least squares lines fitted to the velocity-depth data in Figure 4 show regional trends for the velocity gradients, suggesting that the velocity information can be

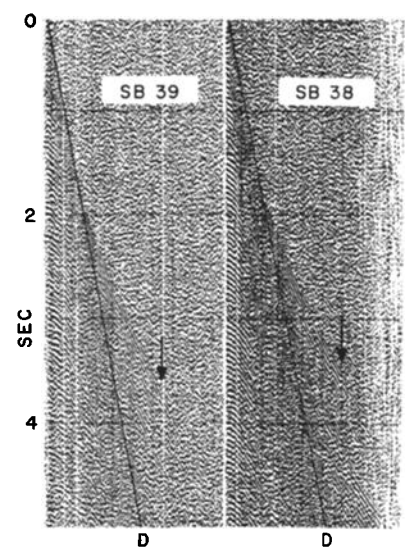

Fig. 3*a*. Examples of sonobuoys showing curvature in the travel time data. The arrows mark the computed range of the limiting ray.

generalized. Although the sonobuoys were deployed in outcrop areas where 2 km of sediment were missing (the beds dip 1°–2° and are truncated), as well as in flat-lying basins, the velocity structures remained invariant. This is implied in Figure 4, where there is no evidence that the 4.4-km/sec material crops out near the surface, even though the reflectors (see Figure 7) show well-defined dips and truncation.

We found on the Ross shelf that the use of the straight-line approximation, where the velocity may actually increase linearly with depth, can lead to thickness solutions that are about 25% less than thicknesses computed from gradients. Another serious shortcoming of the straight-line approximation results from correlating artificial 'constant velocity layers,' which necessarily produces a flat structure section. This would be particularly misleading on the Ross shelf, where dips persist over a large part of the shelf. The data of Figure 4 show that the velocity is overwhelmingly a function of overburden, which rules out velocity as a function of age. Consequently, we have chosen, where it is possible, to compute depths to basement on the assumption of a linear increase of velocity with depth, or $v = v_0 + ah$, where v_0 is the sound velocity at the sea floor, a is the velocity gradient, and h is the depth to the instantaneous velocity v.

Although useful as a diagnostic technique, the plot in Figure 4 cannot be precise because the computed depths based on artificial straight-line refractions are less than the true depths.

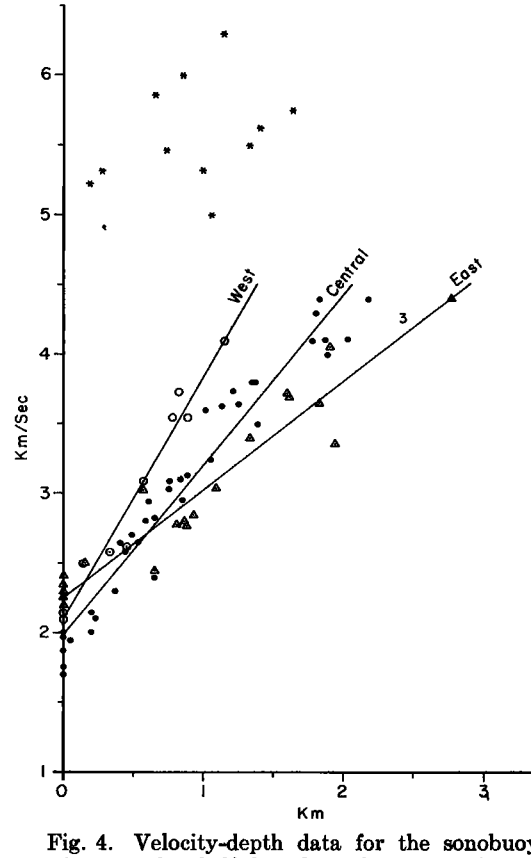

Fig. 4. Velocity-depth data for the sonobuoy stations on the shelf, based on the assumption of constant-velocity layers. Dotted circles, western solutions; solid curves, central solutions; dotted triangles, eastern solutions; asterisk, basement.

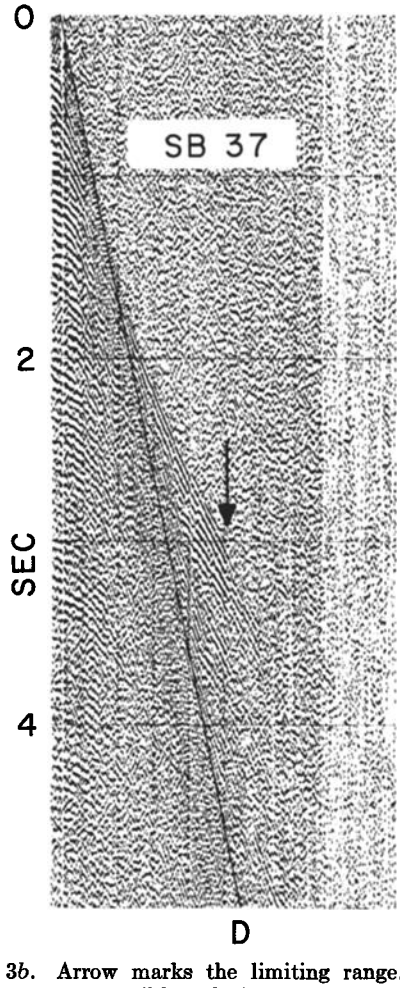

Fig. 3b. Arrow marks the limiting range. Note possible velocity cusp.

We therefore computed velocity gradients from the travel time curves of the original records. The gradients were computed at several different points on each curve in case the gradients changed with depth. The results of this method showed that the velocity gradients (a above) remained constant at all ranges sampled. The results are listed in Table 1. Note that the regional decrease in the velocity gradients toward the east (as seen in Figure 4) is confirmed in Table 1. Average regional values for v_0 and the average regional gradients are listed as the generalized velocity functions at the bottom of Table 1.

TABLE 1. Velocity Gradients from Sonobuoy Travel Time Data

Sonobuoy No.	Gradient, sec^{-1}	Region
3	0.95	Central
4	1.20	Central
37	1.35	Central
38	0.95	Central
39	0.90	Central
7	0.55	East
8	0.65	East
13	0.60	East
30	1.30	West
31	1.20	West
32	1.30	West

Averaged data $v = v_0 + ah$. West: $v = 2.10 + 1.27\ h$; central: $v = 1.98 + 1.07\ h$; east: $v = 2.25 + 0.60\ h$. v_0 obtained from regional averages.

Final solutions appear in Table 2, where the maximum observed velocity in the sediment is used to compute thickness from v_0 and a. Regional gradients were used whenever a reliable gradient could not be obtained, and v_0 was assumed (usually from regional mean values) when it was not measurable on the records. Details of the techniques that were used to find the velocity gradients and to compute the sections appear in the appendix.

There is an unexpected agreement between the maximum thickness of sediments computed from gradients and the depth to basement computed from the basement refraction intercept in those sonobuoys (30–34) where both methods can be applied. We would expect the straight-line calculations to yield a thinner sediment cover on basement than the gradient technique, as they do elsewhere. If anything, the reverse is true at the five stations listed. This could happen if the refracted energy in the sediments attenuates to a level below the noise before the waves return from basement or if the basement head wave propagates somewhat below acoustic basement, a possibility discussed by *Houtz et al.* [1970]. In the structure sections that appear

TABLE 2a. Sonobuoy Solutions from Ross Shelf for Curved Ray Paths

Sonobuoy No.	v, km/sec	v_0, km/sec	a, sec^{-1}	h, km	Basement Velocity, km/sec	Basement Depth, km	Water Depth, km	Location
2	4.30	(1.75)	(0.90)	2.83			0.376	76°54.2'S, 174°47.9'E
3	4.11	1.75	0.95	2.48			0.372	76°58.8'S, 174°48.2'E
4	4.10	1.75	1.20	1.96			0.406	77°06.2'S, 174°49.3'E
7	4.40	2.30	0.55	3.82			0.398	76°20.7'S, 166°25.2'W
8	3.70	2.19	0.65	2.32			0.398	76°25.8'S, 166°49.7'W
13	4.05	2.40	0.60	2.75			0.606	76°12.0'S, 177°28.3'W
14	3.72	(2.25)	(0.60)	2.45			0.591	76°20.7'S, 177°24.4'W
15	3.36	2.26	(0.60)	1.83			0.595	76°28.9'S, 177°18.2'W
18	2.65	(1.98)	(1.07)	0.63			0.462	75°07.2'S, 179°59.3'E
30	3.85	(2.10)	1.30	1.35	5.62	1.50	0.480	75°50.4'S, 173°02.6'E
31	3.75	2.15	1.20	1.33	5.50	1.33	0.494	74°56.1'S, 173°03.0'E
32	4.10	2.10	1.30	1.54	5.76	1.63	0.485	75°03.3'S, 173°03.6'E
33	2.65	1.97	(1.07)	0.64	5.32	1.00	0.266	74°30.1'S, 177°48.2'E
34	3.09	1.87	(1.07)	1.14	5.00	1.06	0.268	74°30.1'S, 177°27.1'E
35	3.80	(1.98)	(1.07)	1.70			0.266	74°30.1'S, 177°01.9'E
36	4.00	(1.98)	(1.07)	1.89			0.265	74°30.2'S, 176°33.1'E
37	4.11	1.70	1.35	1.79			0.398	74°30.2'S, 176°05.3'E
38	4.30	2.00	0.95	2.42			0.441	74°30.2'S, 175°36.8'E
39	4.40	2.14	0.90	2.51			0.482	74°30.4'S, 175°07.9'E

$v = v_0 + ah$, where v is maximum observed velocity in sediments. Parentheses indicate assumed value.

TABLE 2b. Sonobuoy Solutions from Ross Shelf for Straight Ray Paths

Sonobuoy No.	v_1, km/sec	v_2, km/sec	v_3, km/sec	h_1, km	h_2, km	Water Depth, km	Location
6	2.35	5.09		0.74		0.675	77°56.5'S, 178°07.3'W
16	(2.00)	5.32	6.30	0.27	1.44	0.625	77°32.9'S, 179°35.3'W
17	(2.00)	5.22	5.87	0.19	0.65	0.628	77°25.4'S, 179°23.6'W
19	(2.40)	6.00		0.84		0.289	74°29.1'S, 179°49.4'W

$v = v_0 + ah$, where v is maximum observed velocity in sediments. Parentheses indicate assumed value.

later we use the thicker section resulting from the two solutions.

The arrows in Figures 3a and 3b indicate computed range for the limiting ray. In each case the arrow plots very near a point where the energy diminishes rapidly, but a weak signal sometimes continues past the limiting range. In Figure 3b a prominent subbottom event (not observable near vertical incidence) joins the primary refraction curve, very much as if a cusp has formed as the limiting range is approached.

Interval and refraction velocities from the continental rise appear in Table 3. The interval velocities from the sediment layers have been determined by the method described by *Le Pichon et al.* [1968], using variable angle reflection curves. These solutions are shown with a standard deviation. Thicknesses computed from the deeper refraction data were obtained by using water depth, thickness, and mean velocity of the sediment from the interval solutions, apparent refraction velocities, and dip angles (based on the apparent velocities). The program solves for 'true velocities' and uses these values to correct the dip angle and then solves for a 'truer velocity.' The correction is insignificant for dips less than 3°. A small error occurs in the refraction solutions from assuming a mean velocity for the sedimentary column. This error is not likely to be greater than the error that arises by assuming a velocity for the layer between the deepest interval solution and the basement intercept.

A least squares line has been fitted to the interval velocities from the rise to give

$$v = v_0 + kt$$

or

$$v = 1.50 + 2.02t \pm 0.2 \text{ km/sec}$$

where the sea floor sound velocity is 1.5 km/sec (500 m/sec slower than the average sea floor velocity on the shelf), 2.02 km/sec^2 is the acceleration factor, and t is one half the reflection time to the depth of the instantaneous velocity v. The equivalent velocity-depth function is

$$v = (v_0^2 + 2kh)^{1/2} = (2.25 + 4.04h)^{1/2}$$

The different techniques used for the shelf and the rise are a matter of convenience rather than of expressing a fundamental difference in the velocity distributions. Interval velocities from the rise are measured in terms of reflection time,

TABLE 3. Sonobuoy Solutions from the Ross Sea Continental Rise

Station	v_1, km/sec	v_2, km/sec	v_3, km/sec	v_4, km/sec	v_5 (basement), km/sec	Water, km	h_1, km	h_2, km	h_3, km	h_4, km
10	1.72 ± 0.04	2.40 ± 0.04	3.02		4.56	2.15	0.58	0.67	1.42	
11	1.96 ± 0.06	1.99 ± 0.06	2.73 ± 0.05		4.58	2.45	0.41	0.44	1.19	
12	1.78 ± 0.05	2.24 ± 0.09	3.38 ± 0.20	3.48 ± 0.19	4.50	2.90	0.63	0.71	1.14	1.03
24	1.57 ± 0.05	1.98 ± 0.14	3.04 ± 0.12		4.68	2.16	0.49	0.46	0.67	
25	1.88 ± 0.21	3.06 ± 0.10			4.70	2.10	0.95	1.36		
26	1.82 ± 0.04	2.91 ± 0.06	4.00			1.91	0.61	1.42		
27	1.90 ± 0.09	2.55 ± 0.22	3.23 ± 0.22			1.79	0.56	0.61	1.09	
28	(2.00)	2.86	3.53	4.30		1.68	0.87	1.47	0.81	
29	1.93 ± 0.05	2.53 ± 0.06	(3.00)		4.41	1.63	0.49	0.69	1.81	

Parentheses indicate assumed velocities.

whereas the shelf computations lead to answers in units of length (whether we assume $v = v_0 + ah$ or use refraction line slopes and intercepts).

SHELF STRUCTURE

Figure 5 shows the locations of the profiler sections discussed in the text and all the sonobuoy stations.

Dips and strikes on the shelf have been computed from the intersections of profiler tracks by assuming a sound velocity in water of 1.45 km/sec and a near-surface sediment sound velocity of 2.0 km/sec. Results are summarized in Figure 6, where dips and strikes (including a few less reliable solutions based on assumed strikes) and major axial traces of folds are shown. The term 'fold' is used descriptively in this text and does not necessarily imply tectonic activity. For the most part the older fold axes are poorly determined, trend ENE, and are overlain by younger, unconformable basins that plunge out to the north. These structural trends are confirmed by the numerous outcrops that we have observed in the profiler data and appear in Figure 6 as stippled zones. The zones represent what appear to be truncated, dipping beds. Two examples of the truncated beds that crop out along the 175°W meridian are shown in sections C-C′ and D-D′ of Figure 7. Sonobuoy data show that basement (5.1 km/sec) is the reflector, level with the sea floor, that almost crops out at the left in each section. In the region of 172°W the most recent, unconformable cover on the truncated beds is as much as 300 meters thick. The dips are frequently variable with depth, especially near the seaward edge of the shelf east of 180°. For the sake of consistency, the dips shown in Figure 6 are generally the steepest dips, which usually occur at depth.

Sections E-E′ and F-F′ (traced from poor quality profiler data) in Figure 8 reveal minor unconformities along the eastern limbs of the north-trending basins in the western part of the Ross shelf. These unconformities indicate that

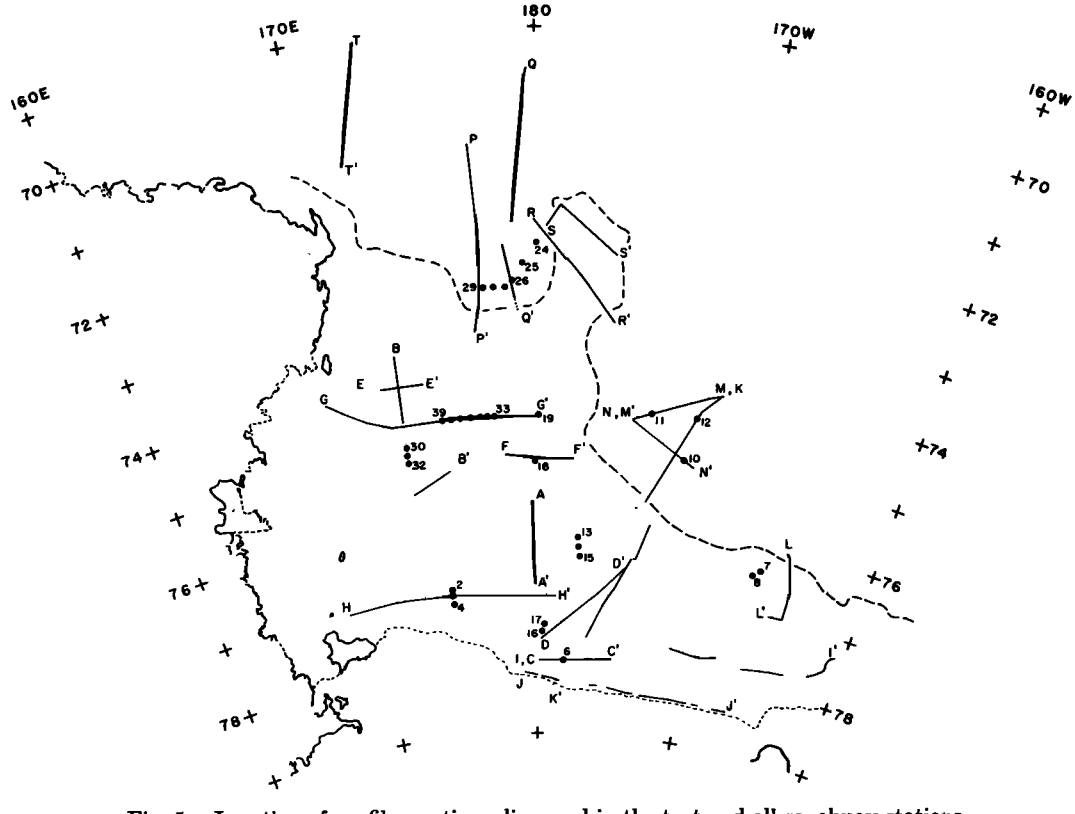

Fig. 5. Location of profiler sections discussed in the text and all sonobuoy stations.

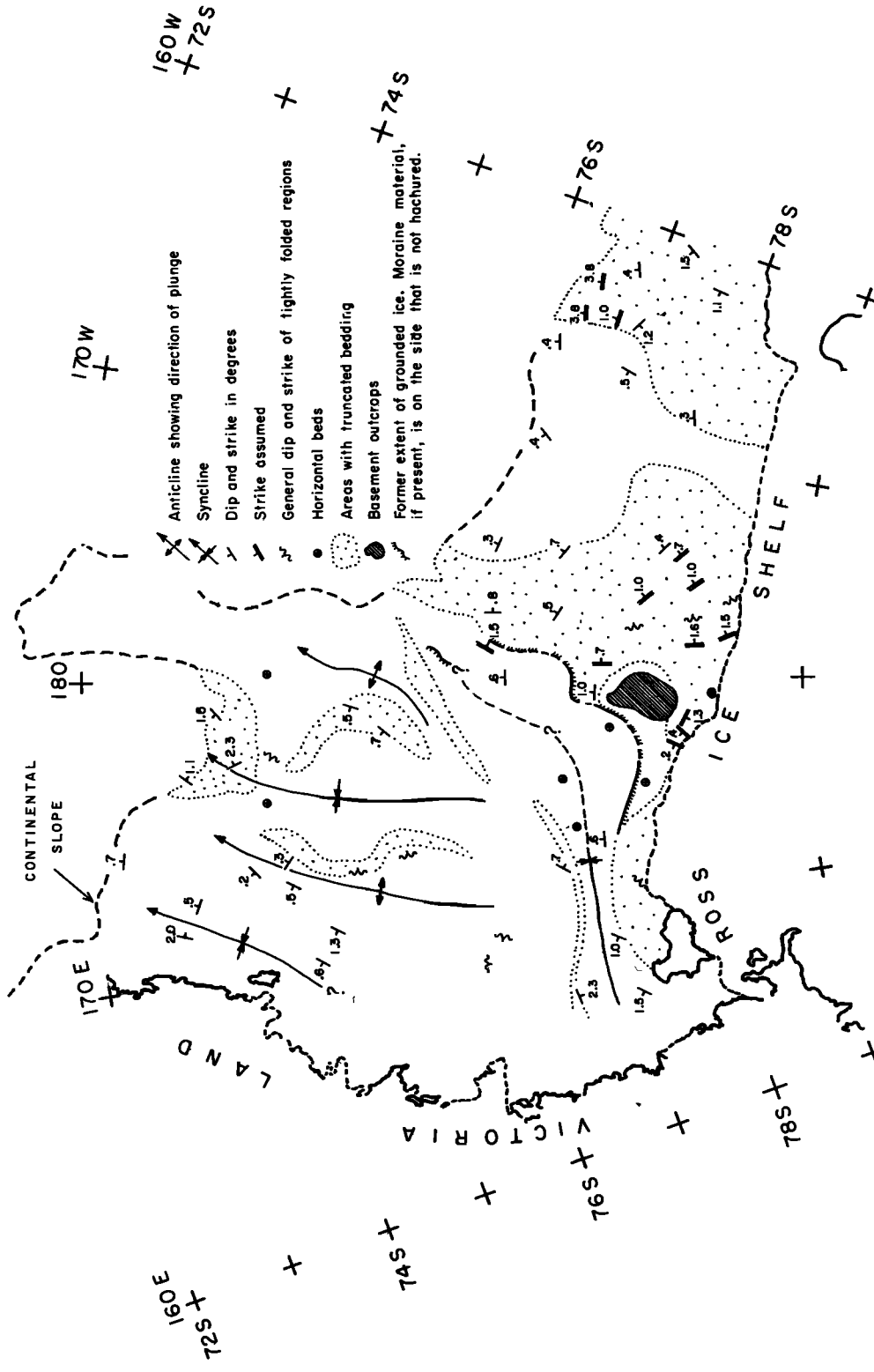

Fig. 6. Near-surface structure of Ross Sea shelf from profiler data.

the basins onlap the underlying beds and therefore provide an explanation for the possibly different sets of folds shown in Figure 6. The data in Figure 8 show that the north-trending basins are probably younger than the ENE fold system.

Structure sections G-G′ and H-H′, accompanied by a photocopy of the profiler data of the former section, are shown in Figure 9. The sections are based on unreversed sonobuoy stations shot end to end (except for station 19, which is a single determination at the eastern end of G-G′). Average sections have been used occasionally when a nearby set of stations does not lie in the plane of the section. Basement refraction velocities shown in the figure have been corrected for dip where necessary.

Section G-G′ requires an abrupt thickening of sediment in the area marked by a normal fault symbol, where the sediment thickens from 1000 to at least 2500 meters. The latter is a minimum depth because basement is not recorded in the central part of the section. The profiler data show no disruption by the presumed fault in the upper 500 meters of sediment, indicating that the fault in the basement is older than the upper sediments. However, the zone of comparatively tight folds beneath the arrow suggests more recent tectonic activity. Tightly folded zones can be identified in Figure 6.

Section H-H′ is similar to G-G′, chiefly in the eastern sector. As in section G-G′, basement refractions are not recorded from the deepest parts of the structure. The proposed fault is poorly defined because no sonobuoys were deployed between the basement outcrops and the central deepest part (measured in sonobuoys 2, 3, and 4). A possible basement high in the west seems to be duplicated in section G-G′, where the depth shown to the 5.6-km/sec basement is the average of results from stations 30, 31, and 32. If sections G-G′ and H-H′ can be correlated, the dips and strikes in the near-surface sediments are quite unrelated to the deep structural trends.

Three sections, I-I′ and J-J′ (east-west) and K-K′ (north-south), across the broad basinal structure indicated in Figure 6 east of 180° are shown in Figures 10 and 11. Section I-I′ shows an east-west composite structure section across

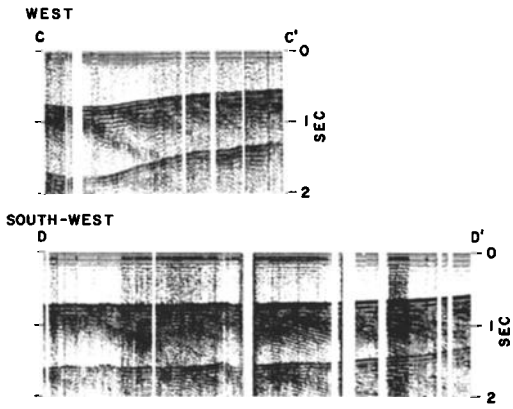

Fig. 7. Profiler records along section C-C′ and D-D′ showing the truncated beds forming the western limb of the basin underlying the eastern Ross Sea.

the basin. In the west, truncated reflectors, with dips from 1.0°E to 1.6°E, can be seen over a distance of about 100 km, thus indicating over 2 km of section in the basin. The truncated reflectors, also shown in sections C-C′ and D-D′ (Figure 7), are covered by up to 300 meters of more recent sediments that appear to form the topographic rise in this region. The upper sediments onlap the underlying beds to the east of this rise. Although the data are not continuous in the area, a similar structure exists on the eastern limb of the basin. Between the two topographic rises the reflectors are subdued and

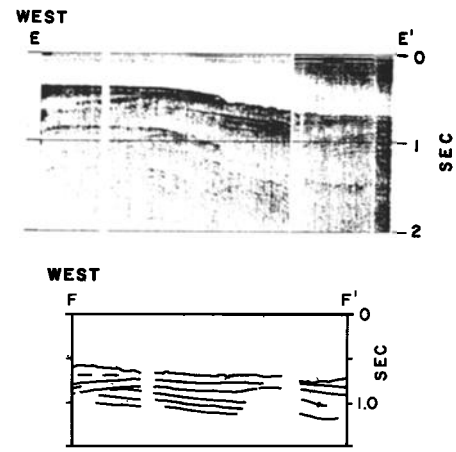

Fig. 8. Profiler record along section E-E′ and line drawing along section F-F′ showing unconformities in the western part of the Ross Sea shelf.

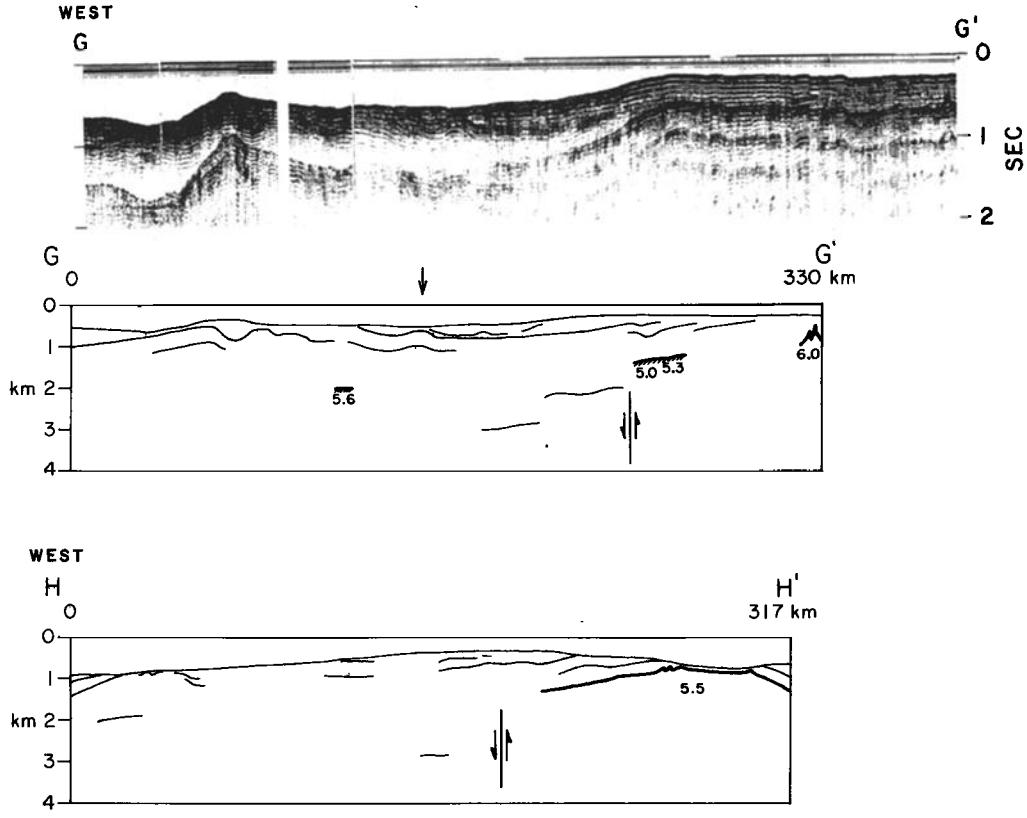

Fig. 9. Structure sections G-G′ and H-H′ based on sonobuoy and profiler data and profiler data along the former section. Note that the scale of the profiler data is in units of time, whereas the line drawings are in units of distance. Basement is indicated by the heavy line, and sonobuoy data by hachured lines.

approximately parallel to the sea floor; thus there is no indication of any major discontinuity in sedimentation in this region. Folding can be seen along both edges of the basin; to the west these folds can be traced roughly north-south, parallel to the edge of the basin. Section J-J′, previously shown in part by *Houtz and Meijer* [1970], is the only profiler record showing postulated basement underlying the central part of the basin. The basement reflector

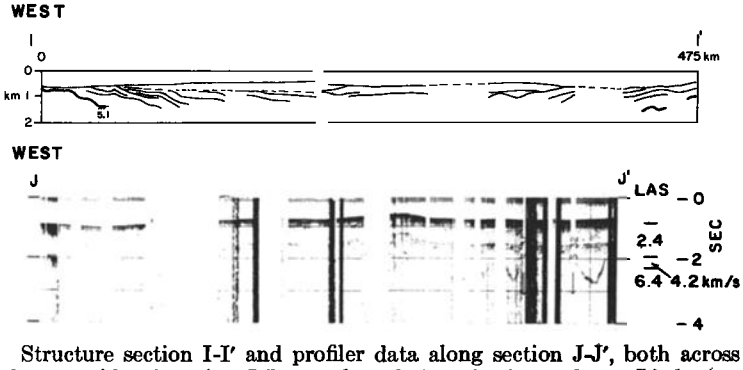

Fig. 10. Structure section I-I′ and profiler data along section J-J′, both across the eastern basin. At the east side of section J-J′ are plotted the seismic results at Little America station [*Crary*, 1962] converted to equivalent two-way reflection time.

shows the existence of large topographic features and the presence of valleys or 'fjords' that deepen by up to 1000 meters below the general basement level. At the western end of the section, like section I-I′, there is a sharp increase in dip of the basement from about 0.5°E to about 1.5°E, which can be taken as marking the western limit of the basin and can be traced roughly northward as far as 76°S. The seismic refraction results of *Crary* [1962] on the sea ice near Little America station, converted into two-way reflection times, are shown at the eastern end of the profile. Although offset by about 100 km to the east of the nearest profiler record showing basement reflection, Crary's data show a depth to basement consistent with the overall basinal structure derived from the reflection data. The upper sedimentary reflectors in section J-J′ show a structure very similar to that seen in section I-I′.

Section K-K′, another composite structure section, runs roughly north-south near the western edge of the basin. The dipping reflectors at the south end of the profile outcrop at an unconformity underlying a thin sediment layer. Further to the north the layers become more nearly parallel to the sea floor. Near the shelf edge the deepest reflectors dip steeply northward, as can also be seen clearly in section L-L′ (Figure 11). The part of section K-K′ that crosses the continental rise will be considered later. Section L-L′, a photocopy of the original profiler record, shows a strong anticlinal structure with a roughly northwest-southeast strike (see Figure 6). This anticline is not seen on any other profiler record in the vicinity. Basement is not seen on the record, but the anticline could be caused by a basement ridge trending northwest from the eastern edge of the basin that plunges or dies out a short distance to the west of section L-L′; it may also represent an isolated dome. The section continues northward from this structure and shows an increasingly steep dip of the reflectors as the shelf edge is approached. At least a 4000-meter thickness of section is indicated at the shelf break.

DISTRIBUTION OF SEDIMENTS ON THE SHELF

Isopachs of sedimentary cover on the shelf together with the simplified land geology of *Craddock* [1972] are shown in Figure 12. Basement, assumed to correspond to seismic velocities greater than 5.0 km/sec on the shelf and

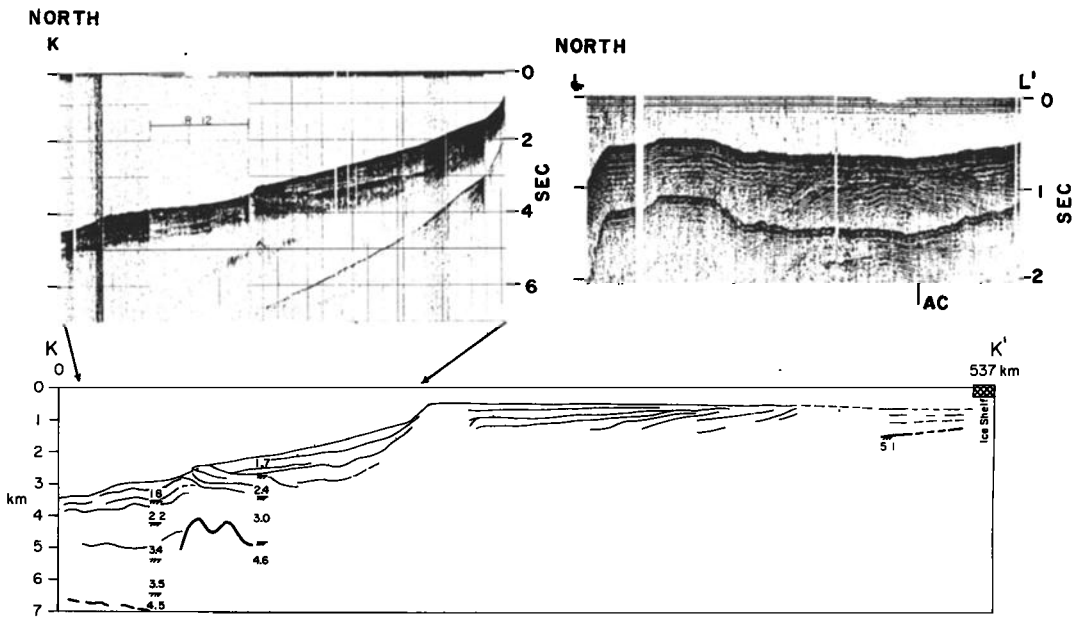

Fig. 11. Structure section K-K′ across the shelf and continental rise in the eastern Ross Sea. The profiler data along the northern part of K-K′ are also shown. Profiler data along section L-L′ show the increasingly steep dips of the deep reflectors toward the shelf edge.

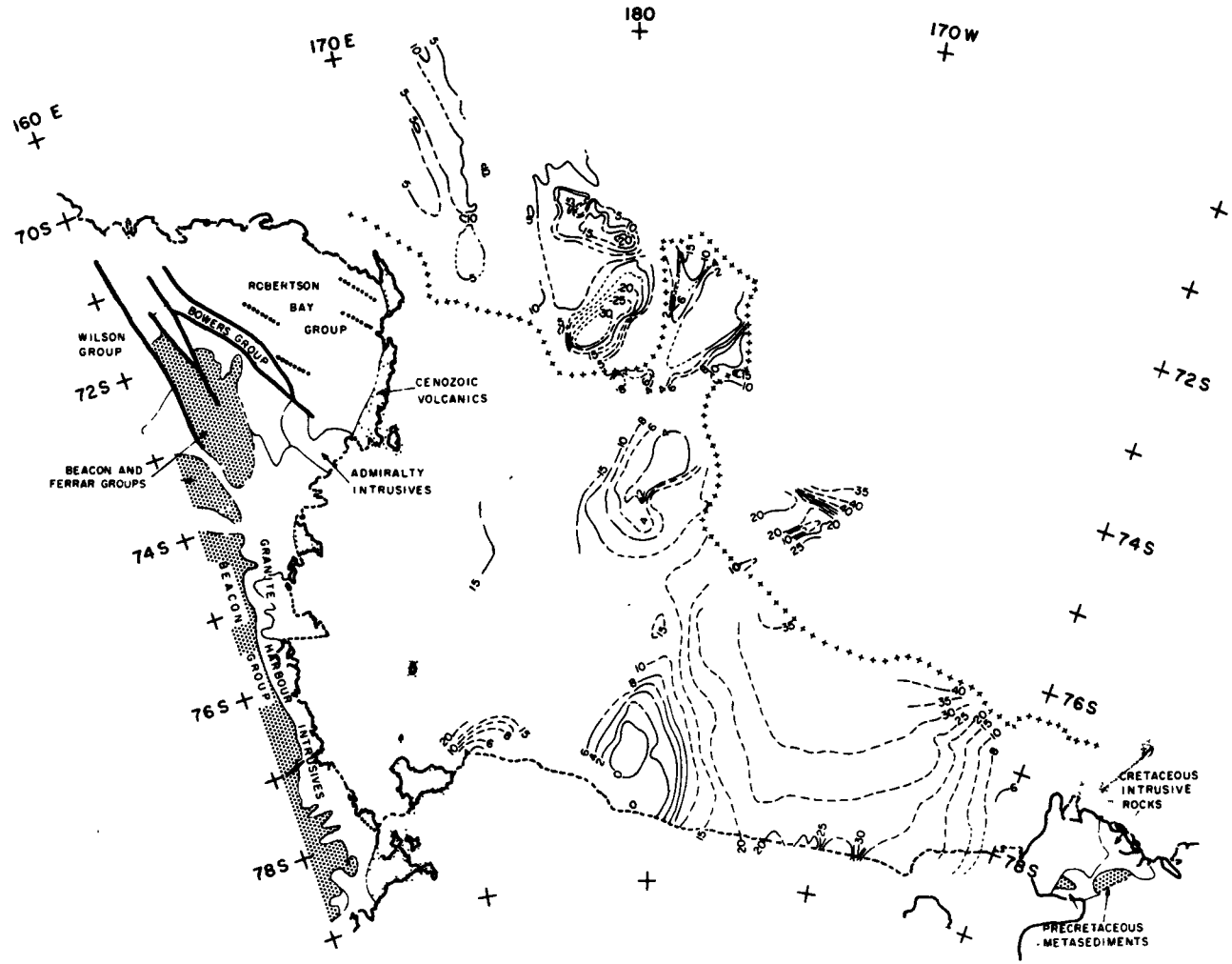

Fig. 12. Sediment isopach map of the Ross Sea with simplified land geology (fold axes shown by dotted lines and faults by heavy lines). Isopachs that are doubtful or extrapolated on the basis of sediment dip are shown as dashed lines. Thicknesses on contours are in 100-meter units.

4.4 km/sec on the rise, is seen only in a few places on the reflection records on the shelf but more frequently on the rise. The basement reflectors are picked by their appearance and position and tend to be confirmed by sonobuoy velocity data where available. Where basement is recorded with confidence, the isopachs are shown by a solid line. In other areas approximate sedimentary thicknesses can be computed by assuming that the thickness of a sedimentary section between two prominent reflectors remains constant with depth. Using this method, the sediment thickness at station 13 (Figure 5), extrapolated from the basement depth of 270 meters at station 16, is 2100 meters compared with an observed 2700 meters from sonobuoy data, and at station 7 an extrapolated sediment thickness of about 4000 meters is obtained compared with an observed 3800 meters. This method has been used to derive the isopachs shown by dashed lines on the shelf east of 180°. To the west of 180°, complexities in the structure of the shelf make it difficult to derive reasonable estimates of minimum sediment thicknesses, and here the dashed lines indicate extrapolation over short distances based on dips seen in the overlying sediments. The isopachs represent a smoothed basement surface, especially where indicated by broken lines; the true basement surface may be far more irregular, as is demonstrated by section J-J′ (Figure 10). The primary features brought out by the isopach map are the broad north-south basin covering the whole of the eastern part of the Ross Sea shelf and the series of basement highs running north-south along 180°. The isopachs for the continental rise and Iselin bank will be discussed next.

RISE STRUCTURE AND ISELIN BANK

Sonobuoy data from the rise are shown in Figure 4 and Table 1; no sonobuoy stations were located on Iselin bank. The profiler data on the rise and bank show, in general, greater penetration than on the shelf. This is partly due to deeper water, which results in less interference from the multiple sea floor reflections.

Data over the rise to the east of Iselin bank are confined to three short connecting profiles, M-M′, N-N′ (Figure 13), and the northern part of K-K′ (Figure 11). Section K-K′ (Figure 11) shows that the upper part of the rise is formed by prograded sediments that are coherent and parallel. They are underlain by a layer that is apparently faulted to the north where it outcrops as a morphological feature toward the bottom of the rise and dips gently southward toward the shelf. This layer corresponds well with the 2.4-km/sec layer seen at station 10. Note that the time-distance curve for sonobuoy 10 is made up of a series of straight lines and not by a continuous curve; hence a correlation with a velocity layer is valid. The outcrop also marks the position of a sharp increase in the depth of basement (velocity 4.6 km/sec) by about 2 km, which is confirmed by the results of stations 10 and 12. The reflections from this deeper basement are discontinuous but can be correlated. Over the deeper basement the upper reflectors are distorted and folded, possibly in-

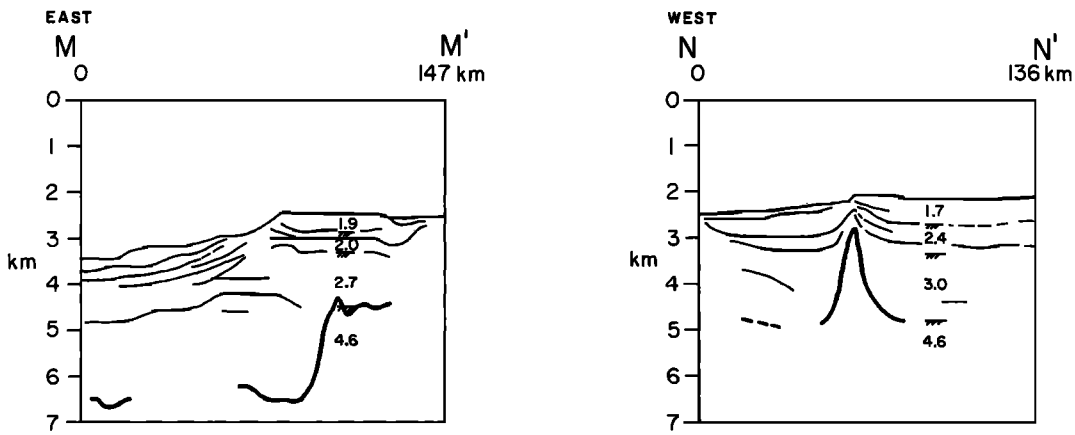

Fig. 13. Structure sections M-M′ and N-N′ over the eastern continental rise.

dicating some degree of slumping. Section M-M′, oriented southwest from the northern end of section K-K′, again shows the sharp increase in depth to basement; this time, however, it is not as closely associated with a surface outcrop layer, although a major morphologic change is evident. Distorted upper sediments are also seen over the deeper basement. Section N-N′ joins the southwestern end of section M-M′, and here the data are not good enough to trace the reflectors clearly, and what reflectors are seen are distorted. Further to the southeast along section N-N′ a basement high is shown whose apparent crest is up to 800 meters below the sea floor. The upper continental rise sediments recorded on section K-K′ are apparently contained to the southeast of this high, which is very similar in shape to a basement rise seen on another profiler track to the southwest and may form a northeast-southwest–trending ridge and barrier to the sediments to the southeast.

The continental rise to the west of 180° is topographically complex (Figure 1*b*). Two north-south sections, P-P′ and Q-Q′ over the eastern part of this rise, are shown in Figure 14. The westernmost section, section P-P′, shows two troughs of sediments up to 3 km thick (as determined from sonobuoy data) separated by a major basement barrier. The southern basin is characterized by smooth flat-lying sediments with only one major reflector at a depth of about 300 meters. The northern basin, however, contains more distorted sediments, associated with a more irregular basement. A small basement high to the level of the sea floor at the north end of this section may block off the flow of these sediments toward the north. Section Q-Q′ shows basically the same features. However, the basement ridge separating the two basins is far narrower here and just approaches the sea floor. The northern edge of the northern basin is formed by a northwest extension of Iselin bank. To the north of Iselin bank up to 700 meters of sediments overlie an irregular basement. Over both sections, basement, apart from basement ridges, lies consistently at a depth of about 4.5 km below sea level to within 50 km of the continental shelf edge. The isopach map (Figure 12) over this part of the continental rise shows that the sediment troughs tend to

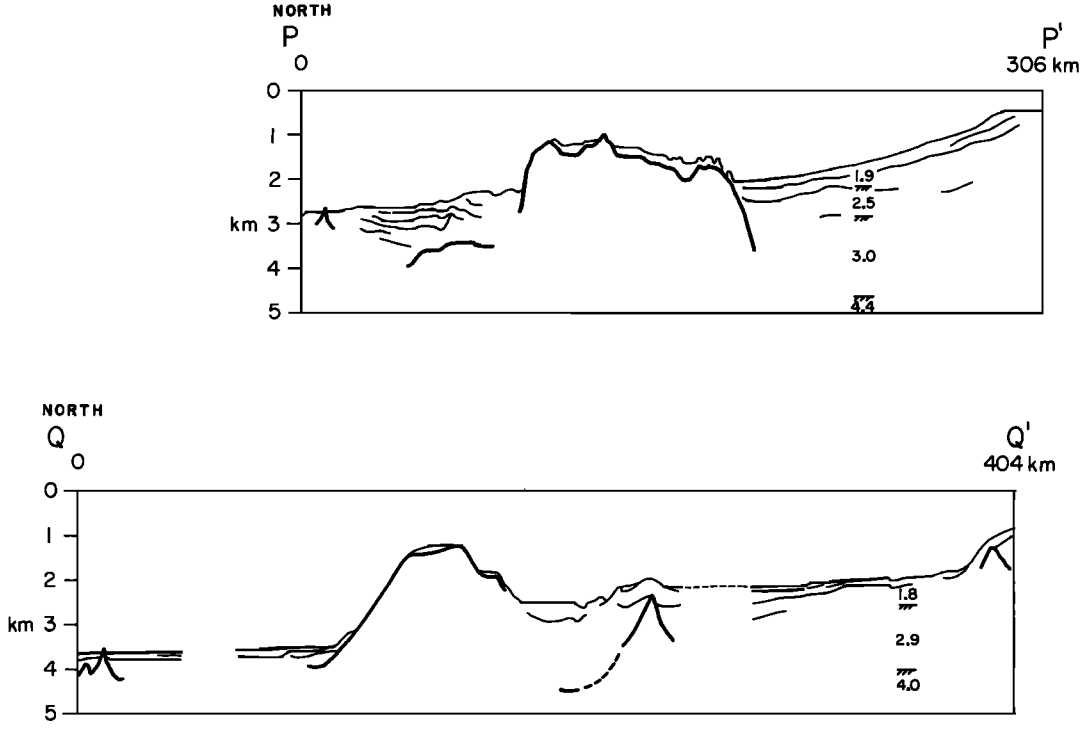

Fig. 14. Structure sections P-P′ and Q-Q′ over the western continental rise.

be elongate and lie parallel to the western edge of Iselin bank. The water depth over the troughs increases to the north, the intermediate basement rise acting as a sediment dam. A fairly swift northward flow of water through the troughs is indicated by the high current velocity measurements at the shelf break [*Jacobs et al.*, 1970]. About 120 km from the continental shelf along 174°E is a V-shaped trough containing about 1.0 km of sediments. It lies on the line of a major graben feature [*Ewing et al.*, 1969] (section T-T′, Figure 15) containing up to 800 meters of sediments and traceable over a distance of 150 km in a NNW-SSE direction.

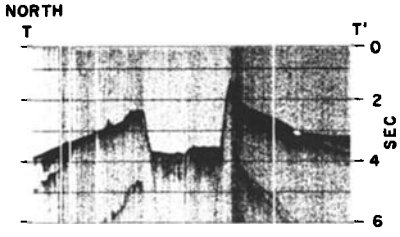

Fig. 15. Profiler record along section T-T′ showing the graben on the western continental rise [after *Houtz and Meijer*, 1970].

Sections R-R′ and S-S′ across the Iselin bank are shown in Figure 16. They, together with the crossing of the bank in section Q-Q′, indicate an asymmetric cross section for the bank. To the north and east of the bank the basement profile is smooth, thick sediments occurring to the southeast where they onlap the acoustic basement. To the south and west the basement profile falls in steps or benches that are partly obscured to the south by sediment cover. Although the data only cover the western part of the bank, in the north they indicate a thinning of sediment cover northward. A marked sediment-filled trough shown in section Q-Q′ apparently splits the bank into two sections.

DISCUSSION

All the dips recorded on the shelf are much less than the natural repose angle of shallow marine sediments, which shows that the present configuration of the sediments on the shelf does not necessitate tectonic control. An exception might be the relatively tight folds that appear within limited areas on the shelf as shown in Figure 6. If the beds had been horizontal on a flat basement at the time of deposition and had remained that way during the consolidation process, the sedimentary velocities would increase in a fairly regular fashion with depth of burial. Later tectonism would then disrupt this pattern, so that the 4.4-km/sec material now recorded deep in the basins should crop out along the flanks of the basement highs. We observe these outcrops in the profiler data, but our velocity determinations in these outcropping layers consistently yield typically low values of about 2.0 km/sec. We therefore favor deposition that was conformable to a previously deformed basement. That is to say, the dips may represent no more than layering parallel to the original basement. However, we cannot discount other possibilities, such as slowly operating chemical processes that have modified the original velocity structure or deposition that occurred contemporaneously with deformation during a relatively short time, but we can definitely rule out any association of sound velocity and age.

The seismic velocity data can be compared with earlier seismic velocity data in the vicinity of the Ross Sea. The seismic data at Little America station have been interpreted in terms of three homogeneous layers of constant velocity [*Crary*, 1962]. Seismic reflection data for the upper low-velocity layer, although assumed to have a constant velocity of 2.4 km/sec, indicate that it has a velocity increasing with depth, from about 2.1 km/sec at the sea floor to about 2.6 km/sec at 900 meters depth. This is not

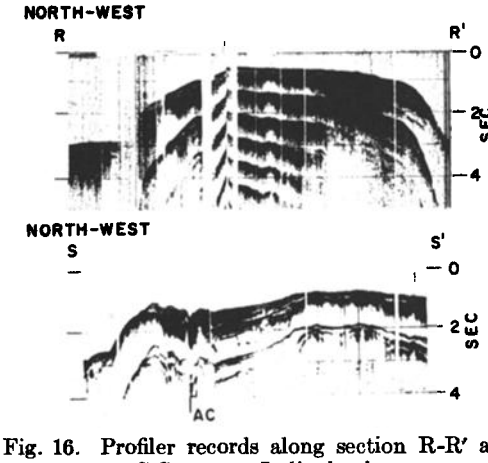

Fig. 16. Profiler records along section R-R′ and S-S′ across Iselin bank.

markedly different from the results of our data further north. The intermediate layer, 4.2 km/sec, is derived from a straight sector of the travel time curve and can thus be assumed to be from a distinct separate layer. This distinct layer with a velocity of about 4.2 km/sec does not fit with our data on the shelf where, as mentioned earlier, seismic velocities of less than the basement velocity (5.1 km/sec or greater) are controlled for the most part by depth of burial. For example, velocities of the order of 4 km/sec are not recorded over basement highs but occur consistently at depth in the deeper sedimentary sections. Thus correlations with the 4.2-km/sec layer at Little America station, tentatively suggested by Crary to be of Beacon group sediments, are difficult. It should be noted that the latter correlation by seismic velocity must be regarded as tentative, as it is based on a seismic measurement at the head of the Skelton glacier about 700 km to the west of Little America station, where the nearest outcrop of the Beacon group sediments is 18 km from the seismic station [*Crary*, 1963]. Seismic velocities of 4.2–4.5 km/sec have been recorded at Camp Wisconsin, 100 km south of Little America station, and at Byrd station [*Bentley and Clough*, 1973]. The variation in depth below the ice at which this layer is seen would seem to preclude any suggestion of it being a permafrost layer in otherwise lower-velocity sediments. *Robinson* [1963] has obtained seismic velocities in the range 3.0–4.8 km/sec near Hut Point on Ross Island. These, however, are interpreted in terms of the local volcanic geology.

The range in basement velocities that we have measured on the shelf, 5.2–6.3 km/sec, suggests a variability that would be expected for metamorphic rocks. Crary's basement velocity of 6.3 km/sec at Little America is not inconsistent with this range. On the Skelton glacier *Crary* [1963] has measured 5.4- and 6.7-km/sec velocities. These he assigns to granitic rocks and Ferrar dolerite sills, respectively. The latter value is significantly higher than any seen on the shelf, and thus one can presume that we have detected none of the Ferrar dolerite sills. The measured velocity range could reasonably be expected to include those for either the pre-Cretaceous rocks of Marie Byrd Land [*Wade and Wilbanks*, 1973] or the Precambrian–lower Paleozoic metamorphic rocks of Victoria Land.

The thin covering of glacial marine sediments on the Ross shelf prevents piston coring devices from reaching the stratified sediments observed on the profiler records. As a result, little stratigraphy is available from the shelf. *Houtz and Meijer* [1970] have already commented on the fjordlike incisions in the basement layer shown in Figure 12 (section J-J′). They suggested that these features may have been formed by Tertiary temperate glaciers [*Denton et al.*, 1970] or by ice movements as early as the Permian [*Lindsay*, 1970; *Frakes and Crowell*, 1970]. The faulted layer at the northern end of section K-K′ (Figure 11) indicates that the lower shelf sediments appear to have been laid down before the separation of New Zealand from Antarctica and should therefore be older than 80 m.y. B.P. [*Christoffel and Falconer*, 1972]. The thickness of the prograded sediments over this faulted layer is in excess of 1 km. Sedimentation rates in this area during the last 3 m.y. have been estimated to be about 1–2 cm/1000 years [*Fillon*, 1972; *Thomas*, 1960]. If this rate is assumed to be a good average value, the faulted layer would be at least 50 m.y. old. The upper surface of the faulted layer appears to be well above basement, which suggests that the oldest sediments on the basement are at least Mesozoic in age. The lack of major glaciation during the Mesozoic apparently limits the age of the fjords in J-J′ to the Cenozoic or the Paleozoic; in view of the thickness of sediments on basement, we favor a late Paleozoic age. Fossiliferous erratics containing Tertiary fossils have been found near Ross Island. Moraines at Minna bluff (McMurdo Sound) yielded gray mudstone erratics containing microfossils of Eocene(?)-Paleocene(?) age [*Harrington*, 1969], and a graywacke found at Cape Crozier (eastern Ross Island) contained fossils assigned to Eocene(?) [*Hertlein*, 1969]. Harrington considers it unlikely that these erratics were derived from west of the Transantarctic Mountains, and thus they must have come from the region now covered by the Ross ice shelf. *Wilson* [1968] has mentioned the existence of lower Tertiary and Permo-Triassic microfossils in Holocene cores from widely spaced positions in the Ross Sea. The Permo-Triassic microfossils were considered to be derived from the Beacon group and present as reworked material in the Tertiary rocks. Recent data from *Eltanin* piston

cores in the Ross Sea [*Fillon*, 1972] have shown the existence of glacial marine deposits older than early Matuyama (2.4 m.y. B.P.) overlain by thin sediments of Brunhes age (up to 0.7 m.y. B.P.). This regional disconformity was considered to be due to increased bottom water erosion associated with an expansion of the Ross ice sheet. The cores are widely spaced over the ridges and valleys on the shelf and over the upper continental rise and indicate a fairly continuous cover of sediments of these ages. The truncated beds seen on the profiler records (for example, Figure 7) are covered in places by up to 300 meters of sediments. Core results indicate that these glacial marine sediments are about 3 m.y. old at depths of up to 10 meters. The age of the unconformity marking the upper surface of the truncated beds is therefore at least 3 m.y. and possibly much older.

The isopach map suggests that the geological structure underlying the Ross Sea can be conveniently considered in two parts separated approximately by the 180° meridian. To the west the geological structure is quite complex and shows large variations in basement topography, whereas to the east there is a broad deep sedimentary basin. The fold structures in northern Victoria Land (see Figure 12) are roughly parallel to the plunging folds mapped in the pre-Cretaceous strata of western Marie Byrd Land. These structures are apparently unrelated to the northerly trend of the basement relief (and younger folds) on the shelf.

The shape of the broad basin to the east as shown on the isopach map is obviously greatly simplified. Data on the Ross ice shelf and Roosevelt Island [*Crary*, 1962; *Bennett*, 1964; *Bentley and Clough*, 1973] indicate that the thick sediments found in this eastern basin probably extend as far as 90°W in the Byrd basin. The minimum depth to basement is 2.5 km below sea level over this region. In the western part of the Ross Sea the velocity-depth curve (Figure 4) shows a sound velocity of about 2.0 km/sec at the sea floor. It would seem reasonable to suggest that the sound velocity of sea floor sediments in the eastern region should be about the same. However, it has the higher value of 2.25 km/sec, suggesting that the basin may have undergone uplift and that the youngest sediments were removed from its surface, possibly by ice erosion or bottom currents. The data in Figure 4 suggest a value of 300 ± 230 meters for the amount of erosion. The low seismic velocity measured at Little America station by *Crary* [1962] could be explained by local conditions, the sediments underlying Little America station being protected partly from the effect of erosion by Roosevelt Island.

Geomagnetic measurements in the southwest Pacific [*Le Pichon*, 1968; *Pitman et al.*, 1968; *Christoffel and Falconer*, 1972], the southeast Indian Ocean [*Weissel and Hayes*, 1972], and the Tasman Sea [*Hayes and Ringis*, 1972] suggest that, before the breakup of Gondwanaland, the Campbell plateau fitted against the eastern Ross Sea margin. *Houtz and Markl* [1972] have remarked on the lack of any suggestion of a marginal rift on the southeast margin of Campbell plateau and suggested that it was a result of an easterly shear away from the eastern Ross Sea. Our data suggest a similar margin for the northern and eastern sides of Iselin bank (section Q-Q′, Figure 14) but show a riftlike structure and major downfault of basement to the north at the base of the eastern Ross Sea continental rise (section K, Figure 11). One is left with two alternatives if the original predrift positions are correct, and these are (1) that the major part of the faulting at the eastern Ross Sea margin is postseparation, possibly associated with the formation of the basin under the eastern shelf, or (2) that the marginal rift remained at the Ross Sea margin after separation. The case for initial shearing between the Campbell plateau and the Ross shelf awaits a more detailed analysis of geomagnetic data. On the other hand, the basement morphology of the western Ross shelf margin matches well with that of the western edge of the Tasmanian platform [*Houtz and Markl*, 1972].

APPENDIX

The equations used for our analysis of the sonobuoy data are based on the assumption that sediment velocities increase from v_0 (km/sec) at the sea floor to some final v (km/sec) at a depth of h (km). Hence

$$v = v_0 + ah \qquad \text{(A1)}$$

where a (sec^{-1}) is the velocity gradient. From the application of Snell's law, the surface-to-surface distance (km) for a refracted ray is

$$X = 2h_0 \tan \theta_0 + (2v_0/a) \cot \theta_1 \quad \text{(A2)}$$

where h_0 is water depth (km), θ_0 is the angle of incidence at the sea surface, and θ_1 is the angle of incidence at the sea floor. The time along the ray is

$$T = (2h_0/v_w) \sec \theta_0 + (2/a) \ln \cot (\theta_1/2) \quad \text{(A3)}$$

where v_w is water velocity. Note that the angles are related by Snell's law:

$$\sin \theta_0/v_w = \sin \theta_1/v_0 = 1/v \quad \text{(A4)}$$

where θ_2 at the bottom of the ray path is 90° ($\sin \theta_2 = 1$).

We could usually measure v_0 on the records, but, when it was not clearly defined, we used average values from the regions shown in Figure 4 or nearby solutions. To find the velocity gradients, we assigned a value of θ_0 (20°–25° was used to produce ranges of about 5 sec of D time (i.e., towards the more distant part of the travel time curves)) and varied a until the difference between the observed and computed T and X values vanished. The gradient can also be determined explicitly by measuring the slope of the travel time curve at a point, but this technique produced more variability and was used only to confirm the gradients determined by trial and error. Equation A4 was also used to compute the range at which the cusp theoretically terminates in the right-hand record of Figure 3; here we use the maximum observed velocity v to compute θ_0 and θ_1 from (A4). These values can then be used in (A2) to compute the range of the assumed limiting ray. This technique does not establish that it is the limiting ray.

Acknowledgments. We are indebted to the officers and crew of the U.S.N.S. *Eltanin* and to the Lamont-Doherty geophysics personnel aboard ship during the Ross Sea cruises. This paper was reviewed by D. Hayes and I. Dalziel, both of whom provided valid criticisms and useful discussions. Cruise 52 was planned in support of the anticipated Deep-Sea Drilling Project and required special logistic efforts by the Office of Polar Programs and the cooperation of numerous scientists in other disciplines to accommodate this special cruise.

The shipboard programs and the research work for this paper were supported by grants from the Office of Polar Programs, National Science Foundation. Dr. Davey was partially supported by the Geophysics Division of the Department of Scientific and Industrial Research, Wellington, New Zealand, during the collection and reduction of the data.

REFERENCES

Adams, R. D., and D. A. Christoffel, Total magnetic field surveys between New Zealand and the Ross Sea, *J. Geophys. Res., 67,* 805–813, 1962.

Bennett, H. F., A gravity and magnetic survey of the Ross ice shelf, Antarctica, *Res. Rep. 64-3,* 97 pp., Geophys. and Polar Res. Center, Univ. of Wis., Madison, 1964.

Bentley, C. R., and J. W. Clough, Seismic refraction measurements of Antarctic subglacial structure, in *Antarctic Geology and Geophysics,* edited by R. J. Adie, University of Forlaget, Oslo, Norway, in press, 1973.

Bryan, G., and E. Simpson, Seismic refraction measurements on the continental shelf between the Orange River and Cape Town, in *The Geology of the East Atlantic Continental Margin, Rep. 70/16,* pp. 187–198, Institute of Geological Science, Cambridge University, Cambridge, 1971.

Calkin, P. E., Glacial geology of the Victoria Valley system, southern Victoria Land, Antarctica, in *Antarctic Snow and Ice Studies II, Antarctic Res. Ser.,* vol. 16, edited by A. P. Crary, pp. 363–412, AGU, Washington, D.C., 1971.

Christoffel, D. A., and R. K. H. Falconer, Marine magnetic measurements in the southwest Pacific Ocean and the identification of new tectonic features, in *Antarctic Oceanology II, The Australian–New Zealand Sector, Antarctic Res. Ser.,* vol. 19, edited by D. E. Hayes, pp. 197–209, AGU, Washington, D.C., 1972.

Chriss, T., and L. A. Frakes, Glacial marine sedimentation in the Ross Sea, in *Antarctic Geology and Geophysics,* edited by R. J. Adie, University of Forlaget, Oslo, Norway, in press, 1973.

Craddock, J. C., Geologic map of Antarctica, Amer. Geogr. Soc., New York, 1972.

Crary, A. P., Marine sediment thickness in the eastern Ross Sea area, Antarctica, *Geol. Soc. Amer. Bull., 72,* 787–790, 1962.

Crary, A. P., Results of United States traverses in east Antarctica 1958–1961, World Data Center, A, *IGY Int. Geophys. Year Glaciol. Rep. Ser., 7,* pp. 69–74, 1963.

Denton, G. H., R. L. Armstrong, and M. Stuiver, Late Cenozoic glaciation in Antarctica, the record in the McMurdo Sound region, *Antarctic J. U.S., 5,* 15–21, 1970.

Eldholm, O., and J. Ewing, Marine geophysical survey in the southwestern Barents Sea, *J. Geophys. Res., 76,* 3832–3841, 1971.

Ewing, M., R. E. Houtz, and J. Ewing, South Pacific sediment distribution, *J. Geophys. Res., 74,* 2477–2493, 1969.

Fillon, R. H., Evidence from the Ross Sea for widespread submarine erosion, *Nature, 238,* 40–42, 1972.

Frakes, L. A., and J. C. Crowell, Geologic evidence for the place of Antarctica in Gondwanaland, *Antarctic J. U.S., 5,* 67–69, 1970.

Harrington, H. J., Fossiliferous rocks in moraines at Minna bluff, McMurdo Sound, *Antarctic J. U.S., 4,* 134–135, 1969.

Hayes, D. E., and J. Ringis, Early opening of the central Tasman Sea, paper presented at International Symposium on the Oceanography of the South Pacific, UNESCO, Wellington, New Zealand, February 1972.

Hertlein, L. G., Fossiliferous boulder of early Tertiary age from Ross Island, Antarctica, *Antarctic J. U.S., 4,* 199–201, 1969.

Hollin, J. T., On the glacial history of Antarctica, *J. Glaciol., 4,* 173–195, 1962.

Houtz, R. E., and R. G. Markl, Seismic profiler data between Antarctica and Australia, in *Antarctic Oceanology II, The Australian–New Zealand Sector, Antarctic Res. Ser.,* vol. 19, edited by D. E. Hayes, pp. 147–164, AGU, Washington, D.C., 1972.

Houtz, R. E., and R. Meijer, Structure of the Ross Sea shelf from profiler data, *J. Geophys. Res., 75,* 6592–6597, 1970.

Houtz, R. E., J. Ewing, and P. Buhl, Seismic data from sonobuoy stations in the northern and equatorial Pacific, *J. Geophys. Res., 75,* 5093–5111, 1970.

Jacobs, S., A. F. Amos, and P. M. Bruchhausen, Ross Sea oceanography and Antarctic bottom water formation, *Deep Sea Res., 17,* 935–962, 1970.

Le Masurier, W. E., Cenozoic volcanic sequence in Marie Byrd Land and its bearing on pre-Pleistocene glaciation in Antarctica, in *Antarctic Geology and Geophysics,* edited by R. J. Adie, University of Forlaget, Oslo, Norway, in press, 1973.

Le Pichon, X., Sea floor spreading and continental drift, *J. Geophys. Res., 73,* 3661–3697, 1968.

Le Pichon, X., J. Ewing, and R. E. Houtz, Deep-sea sediment velocity determination made while reflection profiling, *J. Geophys. Res., 73,* 2597–2614, 1968.

Lepley, L., Submarine geomorphology of the eastern Ross Sea and Sulzberger Bay, 'Antarctica,' *Tech. Rep. 172,* U.S. Naval Oceanogr. Office, Washington, D.C., 1966.

Lindsay, J., Depositional environment of Paleozoic glacial rocks in Transantarctic Mountains, *Geol. Soc. Amer. Bull., 81,* 1149–1172, 1970.

Matthews, D., *Tables of the Velocity of Sound in Pure Water and Sea-Water,* Hydrographic Department, Admiralty, London, 1939.

Pitman, W. C., III, E. M. Herron, and J. R. Heirtzler, Magnetic anomalies in the Pacific and sea floor spreading, *J. Geophys. Res., 73,* 2069–2085, 1968.

Robinson, E. S., Geophysical investigations in McMurdo Sound, Antarctic, *J. Geophys. Res., 68,* 257–262, 1963.

Thomas, C. W., Late Pleistocene and Recent limits of the Ross ice shelf, *J. Geophys. Res., 65,* 1789–1792, 1960.

Wade, F. A., and J. R. Wilbanks, Geology of Marie Byrd and Ellsworth Lands, in *Antarctic Geology and Geophysics,* edited by R. J. Adie, University of Forlaget, Oslo, Norway, in press, 1973.

Weissel, J. K., and D. E. Hayes, Magnetic anomalies in the southeast Indian Ocean, in *Antarctic Oceanology II, The Australian–New Zealand Sector, Antarctic Res. Ser.,* vol. 19, edited by D. E. Hayes, pp. 234–249, AGU, Washington, D.C., 1972.

Wilson, G. J., On the occurrence of fossil microspores, pollen grains and microplankton in the bottom sediments of the Ross Sea, Antarctica, *N.Z. J. Mar. Freshwater Res., 2,* 381–389, 1968.

(Received November 16, 1972;
revised January 29, 1973.)